High-Repetition-Rate Pulsed-Pump Fiber OPA for Amplification of Communication Signals

Georgios Kalogerakis, *Student Member, IEEE*, Katsuhiro Shimizu, *Member, IEEE*, Michel E. Marhic, *Senior Member, IEEE*, Kenneth Kin-Yip Wong, *Member, IEEE*, Katsumi Uesaka, *Member, IEEE*, and Leonid G. Kazovsky, *Fellow, IEEE*

***Abstract*—The use of a high-repetition-rate pulsed-pumped fiber optical parametric amplifier (OPA), followed by a narrow optical filter for transparent signal amplification, was proposed. Theory and simulations predict larger gain and gain bandwidth compared to a continuous-wave pump with the same average power. Experimentally, when using a pump with 0.63 W of average power in a 500-m-long highly nonlinear fiber, the gain increased from 19.7 to 29.2 dB, and the bandwidth increased when a CW pump was changed to one that is modulated by a 20-GHz cosine-squared function. Clear eye openings were demonstrated for the amplification of a 10-Gb/s NRZ signal, with a power penalty of 1.5 dB.**

***Index Terms*—Optical amplifier, optical parametric amplifier (OPA), pulsed pump, pulsed reshape.**

I. Introduction

FIBER optical parametric amplifiers (OPAs) are promising because of their large and flexible gain bandwidth [1]–[5]. Operation of fiber OPAs with continuous-wave (CW) pumps would be desirable for many practical applications. This would provide gain or idler conversion efficiency independent of time, which is convenient for amplifying or converting input signals with arbitrary modulation formats. However, highly nonlinear fibers available today have a zero-dispersion wavelength λ_0, which can vary by several nanometers over a few hundred meters [6]–[8]. This in turn prevents the phase-matching condition from being maintained at its optimum value along the fiber. As a result, to date, CW fiber OPAs have not exhibited gain spectra as wide as that predicted by the standard OPA theory, which assumes a fiber with constant λ_0. In contrast, by using a pulsed pump, which consists of high-peak-power pulses, and a relatively short fiber, one can obtain very wide (> 200 nm) gain spectra, with a shape very close to that predicted by theory [1], [2].

Manuscript received February 3, 2005; revised May 1, 2006. This work was supported in part by the National Science Foundation under Grant ANI-0123441.

G. Kalogerakis, M. E. Marhic, and L. G. Kazovsky are with the Department of Electrical Engineering, Stanford University, Stanford, CA 94305 USA (e-mail: gkalog@stanford.edu).

K. Shimizu was with the Department of Electrical Engineering, Stanford University, Stanford, CA 94305 USA, on leave from the Information Technology Research and Development Center, Mitsubishi Electric Corporation, Kamakura 247-8501, Japan (e-mail: shimi@isl.melco.co.jp).

K. K.-Y. Wong is with the Department of Electrical and Electronic Engineering, University of Hong Kong, Pokfulam, Hong Kong.

K. Uesaka was with the Department of Electrical Engineering, Stanford University, Stanford, CA 94305 USA, on leave from Sumitomo Electric Industries Ltd., Yokohama 244-0844, Japan.

Digital Object Identifier 10.1109/JLT.2006.878012

Thus, we see that using a pulsed pump makes it much easier to obtain wide gain spectra with predictable shapes. Unfortunately, the use of a pulsed pump means that the amplified signals cannot, in general, maintain their original format because the gain will not be constant in time but will occur only during the pump pulses. The resulting amplitude modulation of the signal appears to make this approach unsuitable for arbitrary signal formats.

Here, we present a method that makes it possible to use a pulsed-pump OPA for signals with arbitrary modulation formats by using a high-repetition-rate pulsed-pump OPA followed by a narrowband optical filter. As a result, this arrangement works as a CW OPA but with a larger gain and gain bandwidth, which is determined by the peak power used rather than by the average power. In this paper, we demonstrate a 90-nm bandwidth and low-penalty amplification of 10-Gb/s nonreturn-to-zero (NRZ) signals using a 20-GHz pulsed-pump OPA. Asynchronous pulses can also be utilized, which is essentially required to amplify signals in practical systems.

II. Theory of High-Repetition-Rate Pulsed-Pump OPA

We first introduce the principle of operation by means of an example shown in Fig. 1. The pulsed pump at $\lambda_{\rm p}$ is intensity-modulated (IM) at 20 GHz [Fig. 1(a)]. The input signal at $\lambda_{\rm s}$ is NRZ-modulated at 10 Gb/s [Fig. 1(b)]. The amplified signal [Fig. 1(c)] is the product of the input signal and the periodic gain, which is a waveform with the same period as the pump.

The signal and pump input spectra are shown in Fig. 1(e). Since the pump is periodic in the time domain, its spectrum consists of evenly spaced delta functions. The spectrum of the output signal is the convolution of the spectrum of the input signal and that of the periodic gain; therefore, it consists of equally spaced replicas of the input signal spectrum [Fig. 1(f)].

The narrowband optical filter then selects the central lobe of that spectrum, resulting in the waveform of Fig. 1(d), which closely resembles that of Fig. 1(b), indicating that the pulsed-pump OPA is suitable for amplification of modulated communication signals.

We now turn to the quantitative calculation of the signal gain. We consider a pump with average power $P_{\rm av}$. If the pump is CW, then the maximum gain is well approximated by $G_{\rm cw} = 8.6\,\gamma P_{\rm av} L - 6$ (in decibels), where γ is the fiber nonlinearity coefficient, $P_{\rm av}$ is the average pump power, and L is the fiber length. In our experiments, $\gamma = 11$ W^{-1} km^{-1}, $P_{\rm av} = 0.631$ W, and $L = 500$ m, which yields $G_{\rm cw} = 23.85$ dB. If

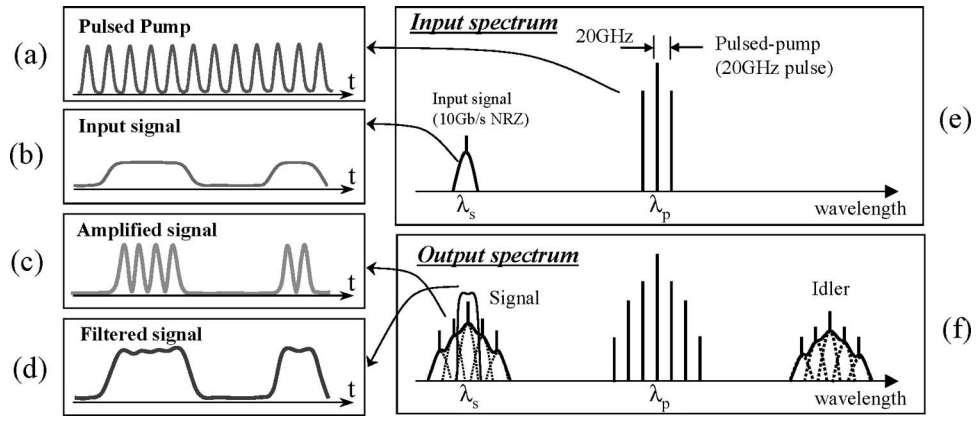

Fig. 1. Principle of operation of the high-repetition-rate pulsed-pump OPA.

the pump is modulated by a square wave, its peak power is $P_{\max} = 2P_{\text{av}}$. If the input signal is CW, the output signal is a square wave. To find the power in the central lobe of its optical spectrum, we must consider the envelope of the output signal field (proportional to the square root of instantaneous power, i.e., also a square wave), find its average value, and then square it. Altogether, this yields a signal power gain $G_{\text{pulse}} = 2\,G_{\text{cw}} = 47.7$ dB for the aforementioned parameters. Hence, we see that if we could implement square-wave modulation of the pump, we could expect to double the signal gain, which would provide a very significant increase.

In reality, it is clearly not practical to implement precisely square-wave modulation of the pump. For example, if we consider a pump modulated at 20 GHz, we might need to use up to ten harmonics in order to have a good approximation of a square wave. This would imply a bandwidth of 200 GHz for the modulation electronics, which is not practical. In practice, it is thus more likely that the pump modulation waveform will occupy a much smaller spectrum and will thus exhibit rounded edges.

Calculating the signal gain for such pump modulation is considerably more complicated than for a square wave. For this reason, we do not provide a closed-form solution. Instead, we have performed numerical simulations using OptSim [9]. Fig. 2 shows results of simulations performed for different types of pump modulation waveforms and a CW signal. We used a raised-cosine function, whose shape can be varied by changing the rolloff parameter ρ; $\rho = 0$ corresponds to a square wave, whereas $\rho = 1$ corresponds to cosine-squared modulation, which is the least demanding for the modulation electronics. Intermediate values of ρ give waveforms that look like square waves with rounded edges, which can provide good models for practical waveforms. For comparison, we have also shown in Fig. 2 the gain curve for a CW pump. We verify that, as previously shown, square-wave modulation should provide a large increase in maximum gain. On the other hand, cosine-squared modulation provides a smaller gain improvement. The reason for the difference is qualitatively clear: For a square wave, the pump power spends a full half-period at $P_{\max} = 2P_{\text{av}}$, whereas for cosine-squared modulation, it only reaches $P_{\max}$ at one instant during one half-period.

The maximum gain obtained by numerical simulation does not quite match that obtained by simple analytical calculation. There are two possible reasons for this, due to effects that are present in OptSim but not in the simple formula: 1) stimulated Raman scattering, which is responsible for the slight asymmetry of the spectrum [1]; 2) gain saturation, which may occur even for low signal input power when high gains are obtained; and 3) modification of the pump spectrum by modulation instability.

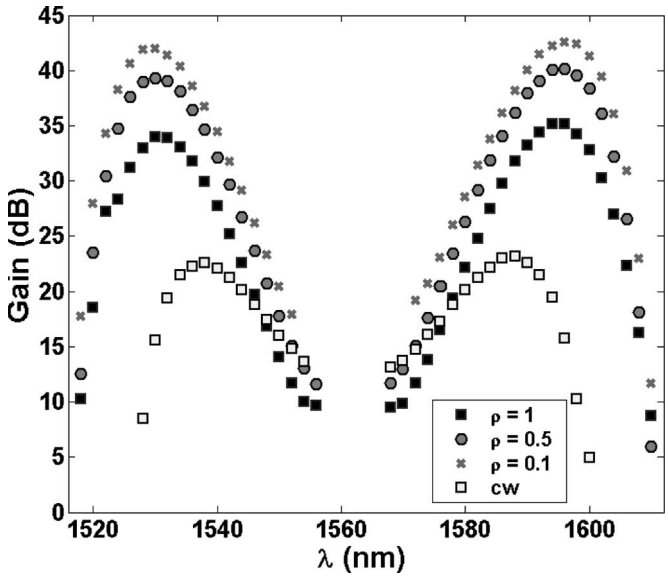

Fig. 2. Gain spectra obtained by OptSim simulations (average pump power: 28 dBm; signal input power: −35 dBm; pump wavelength: 1561.96 nm; fiber loss: 0.5 dB/km; fiber nonlinear coefficient: $\gamma = 11\ \text{km}^{-1}\text{W}^{-1}$; zero-dispersion wavelength: $\lambda_0 = 1561.14$ nm; dispersion slope: 0.03 $\text{ps}/(\text{nm})^2/\text{km}$; fourth-order dispersion parameter: $\beta_4 = -5.8 \cdot 10^{-5}\ \text{ps}^4\text{km}^{-1}$).

Let us now turn to the gain bandwidth, which we define as that region over which there is appreciable signal gain. For a CW fiber OPA made from a uniform fiber and $\lambda_{\text{p}} = \lambda_0$, the gain bandwidth (on one side of λ_0 only) is

$$\Delta\lambda_4 = \frac{\lambda_0^2}{\pi c}\left(\frac{3\gamma P_{\text{av}}}{-\beta^{(4)}}\right)^{1/4} \tag{1}$$

where c is the speed of light in vacuo, and $\beta^{(4)}$ is the fourth-order dispersion coefficient [3]. The fourth-root dependence of $\Delta\lambda_4$ on power indicates that for a pump modulated by a square

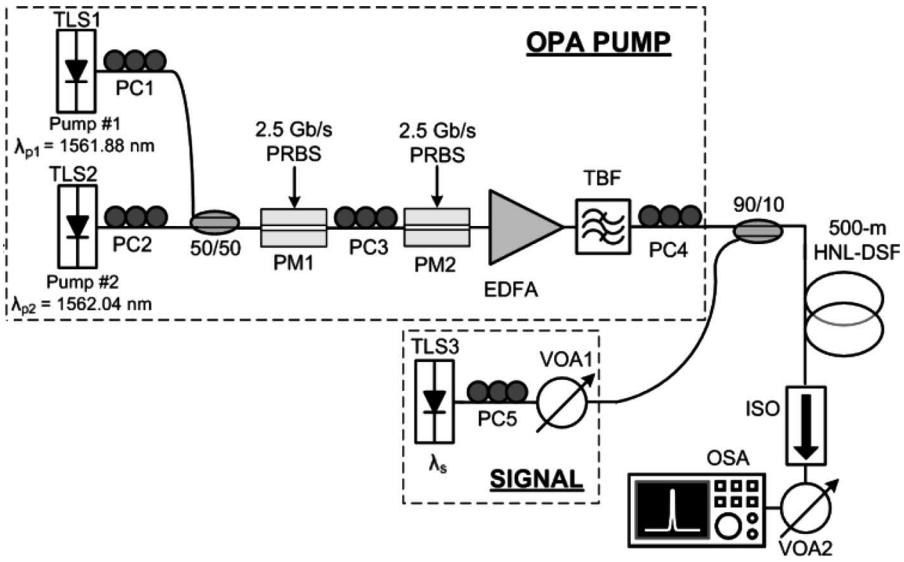

Fig. 3. Setup for signal gain measurements (TLS, tunable laser source; PC, polarization controller; PM, phase modulator; EDFA, erbium-doped fiber amplifier; TBF, tunable bandpass filter; HNL-DSF, highly nonlinear dispersion-shifted fiber; ISO, isolator; VOA, variable optical attenuator; OSA, optical spectrum analyzer).

wave, with peak power equal to $2P_{\rm av}$, $\Delta\lambda_4$ will be increased by $2^{1/4} = 1.19$, i.e., by a modest amount. This is in agreement with Fig. 2.

We also note in Fig. 2 that all the modulated waveforms have the same gain bandwidth. This is due to the fact that they all have the same peak power $P_{\max} = 2P_{\rm av}$. If we think of the expression for $\Delta\lambda_4$ as being applicable on an instantaneous basis, with the instantaneous power replacing $P_{\rm av}$, we conclude that the instantaneous $\Delta\lambda_4$ reaches but never exceeds $\Delta\lambda_4(P_{\max})$. As a result, looking over one period, there is always some gain for wavelengths within that range but none outside; hence, the gain bandwidth is always given by $\Delta\lambda_4(P_{\max})$ regardless of the actual waveform, which is in agreement with Fig. 2.

In a real fiber, λ_0 is not uniform but varies along the fiber length. As a result, the maximum gain will generally be smaller than that in a uniform fiber, and the shape of the gain spectrum will be different. The gain bandwidth may be smaller or larger than $\Delta\lambda_4$, depending on where $\lambda_{\rm p}$ is located with respect to the distribution of λ_0 in the fiber. At larger pump powers, however, the nonlinear phase-matching terms become relatively large compared to the linear ones, and therefore, variations in the latter ones induced by λ_0 variations play a less important role. Therefore, as pump power is increased, gain spectra should tend to look more like those in uniform fibers.

III. Gain Measurements

We first performed signal gain measurements in order to check the predictions of the preceding theory. We did not use signal modulation, as it was not necessary at this stage. The experimental setup is shown in Fig. 3. The parametric gain medium consisted of 500 m of highly nonlinear dispersion-shifted fiber (HNL-DSF) from Sumitomo Electric Industries, Ltd., with nominal $\lambda_0 = 1561.14$ nm, a dispersion slope of 0.03 ps/nm^2, and $\gamma = 11$ W^{-1} km^{-1}.

The pump consisted of two tunable laser sources TLS1 and TLS2 set at $\lambda_1 = 1561.88$ nm, and $\lambda_2 = 1562.04$ nm (i.e., about 20 GHz apart), respectively, and combined by means of a 3-dB coupler. The sum of these two waves is equivalent to a single carrier at $(\lambda_1 + \lambda_2)/2$, with cosine-squared IM at the frequency $f_{\rm m} = c(1/\lambda_1 - 1/\lambda_2) = 20$ GHz, and 100% modulation depth (i.e., the raised-cosine function of Section II, with $\rho = 1$) [10]. This method provides a pump with well-characterized IM, which can be used for accurate comparison with the theoretical predictions of Section II.

The CW pumps were also phase-modulated by a 2.5-Gb/s $2^7 - 1$ pseudorandom bit sequence (PRBS) to suppress stimulated Brillouin scattering (SBS). Two phase modulators PM1 and PM2 were cascaded to obtain a high Brillouin threshold. Polarization controllers PC1 and PC2 aligned the pump's state of polarization (SOP) with PM1, whereas PC3 aligned it with PM2, which helped to reduce the insertion loss.

The signal was provided by another tunable laser source TLS3. The OPA gain was maximized by aligning the SOP of the pump with that of the signal by PC4 and PC5. The signal was combined with the pump by a 90/10 coupler, and the two then entered the HNL-DSF.

The output of the HNL-DSF was attenuated, and the optical spectrum was observed on the Optical Society of America (OSA). When observed with a high resolution, the spectra of the pump, signal, and idler were seen to consist of a few narrow peaks, which are separated by 20 GHz, as expected. In order to measure the signal gain defined in Section II, it was necessary to select only the central peak of the signal spectrum; we found that an OSA resolution of 0.1 nm was suitable. Fig. 4 shows the signal gain spectrum measured in this manner, with a total average pump power of 28 dBm (631 mW). For comparison, we also repeated the measurement with a CW pump, with the same power (in all cases, the gains were ON–OFF gains, i.e., the difference in decibels between the signal output powers with the pump on or off).

As expected from Section II, we indeed observe that the gain spectrum is improved in two key respects by using a pulsed pump instead of a CW one. We first note that the maximum

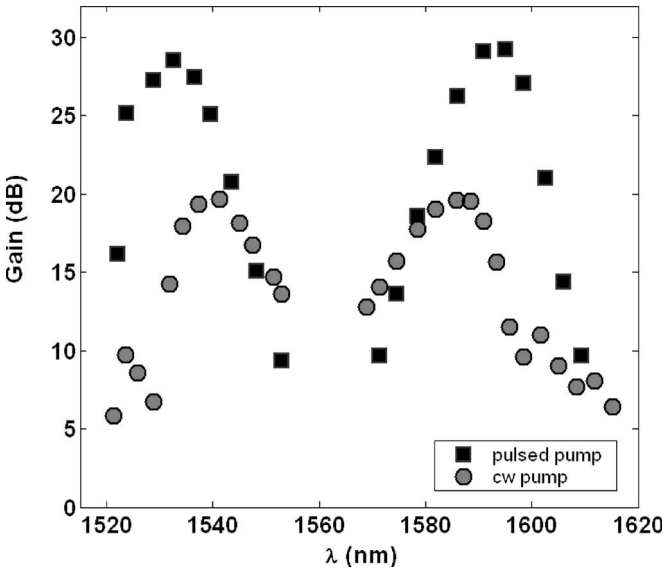

Fig. 4. Experimental OPA gain spectra for both CW and pulsed-pump cases (average pump power: 28 dBm; signal input power: −30 dBm; center pump wavelength: 1561.96 nm; fiber loss: 0.5 dB/km; fiber nonlinear coefficient: $\gamma = 11\ \mathrm{km}^{-1}\mathrm{W}^{-1}$; zero-dispersion wavelength: $\lambda_0 = 1561.14$ nm; dispersion slope: 0.03 $\mathrm{ps}/(\mathrm{nm})^2/\mathrm{km}$; fourth-order dispersion parameter: $\beta_4 = -5.8 \cdot 10^{-5}\ \mathrm{ps}^4\mathrm{km}^{-1}$).

gain is increased from 19.7 to 29.2 dB. We also note that the gain spectrum looks wider. However, because the definition of bandwidth is not unique, it is somewhat difficult to quantify the improvement unambiguously.

Comparing with the theoretical plots of Fig. 2, we see that there is fairly good agreement between the pulsed spectra. On the other hand, for the CW spectra, the experimental one is far worse than the theoretical one. These observations are in good qualitative agreement with the types of gain spectra expected in a fiber with significant longitudinal variations of λ_0, as we discussed in Sections I and II: CW experimental spectra generally look worse than the theoretical ones, but the difference is reduced for pulsed spectra (with higher peak pump power).

IV. Performance Measurements

We then performed experiments to investigate the system-level performance of the technique, with the carrier now being modulated by a binary NRZ communication signal. The experimental configuration is shown in Fig. 5. We describe in detail only those parts that are different from those in Fig. 3.

The tunable laser source TLS1, which is set at 1561.96 nm, served as the single pump source. It was IM by two electroabsorption modulators (EAMs) (we used EAMs here instead of two CW pumps to try and better approximate square-wave modulation because it can provide better performance, as shown in Section II). The duty cycle used was 20%, which corresponds to 7 dB of modulation loss. Each EAM also had another 10 dB of insertion loss; hence, the total loss incurred in the two cascaded EAMs was 27 dB. A C-band EDFA (EDFA1) was placed between the two EAMs to compensate for their large induced loss. The EAMs were driven by a 10-GHz clock from the pattern generator. The pump after the EAMs thus became a 10-GHz train of pulses, with full-width at half-maximum (FWHM) of about 15 ps. It was amplified by EDFA2 and filtered by a 3-nm bandwidth tunable bandpass filter TBF1 to reduce the amplified spontaneous emission (ASE) noise. It was then optically multiplexed by an optical delay line (ODL) and two 50/50 couplers to form a 20-GHz pulse train (with a 40% duty cycle). PC3 and PC4 helped to align the SOPs in the two branches, while VOA1 and VOA2 were used to equalize their powers. The pump was further amplified by EDFA3, which had a maximum output power of 3 W. TBF2 was a high-power tunable bandpass filter with a 3-nm bandwidth used to reduce the ASE noise of EDFA3.

The signal was again provided by TLS3, which is now modulated by a 10-Gb/s NRZ $2^{23} - 1$ PRBS. Amplification by EDFA4 saturated the OPA gain, which helped suppress the noise in the mark level. The output spectrum of HNL-DSF was filtered by a circulator and fiber Bragg grating (FBG) filter, which had a passband width of 0.158 nm. The FBG and circulator had insertion losses of 0.5 dB and 1 dB, respectively. Because the dispersion of the FBG was about 1000 ps/nm, we used about 60 km of single-mode fiber (SMF) to compensate it. The SMF (not shown in Fig. 5) was placed just after the circulator and before the EDFA5. Its total loss was 12 dB. Eye diagrams and bit-error-rate (BER) curves were measured with the digital communication analyzer (DCA) and BER tester, respectively.

The performance of the pulsed-pump OPA is shown in Fig. 6. The eye patterns with synchronous pump, where the 20-GHz pulsed pump was synchronized with the 10-Gb/s signal, are shown on the left. Fig. 6(a) is the waveform before the FBG filter. It shows that the input 10-Gb/s NRZ signal was sampled at 20 GHz by the pulsed OPA. After passage through the FBG, the 20-GHz spectral component was rejected, and the 10-Gb/s NRZ signal was recovered, as shown in Fig. 6(b).

In order for this OPA to amplify input signals transparently, a narrowband optical filter is necessary. However, if a pulsed-pump OPA is used as preamplifier for an optical receiver, an electrical lowpass filter can be a good alternative to the narrowband optical filter. Fig. 6(c) shows the received signal waveform obtained by using an electrical lowpass filter instead of the narrowband optical filter.

In Fig. 6(b) and (c), the residual 20-GHz ripple is due to the imperfect characteristics of the available filters; it could be reduced by using better filters.

BER plots for the output signal, which correspond to Fig. 6(b), are shown in Fig. 7. Although a penalty of 1.5 dB was observed, error-free operation was confirmed, which proves the feasibility of using the pulsed-pump OPA for amplifying NRZ signals. The penalty is thought to result mainly from the imperfections of the optical filter characteristics, i.e., its bandwidth, dispersion, and dispersion ripple.

Note that when we measured the BER, the input signal power was raised to about 1 dBm, which reduced the gain by saturation (pump depletion) to 8.5 dB. This improved the optical signal-to-noise ratio (OSNR) and the BER because signal intensity fluctuations are reduced when the gain is saturated [11].

Asynchronous pumping was also investigated, where the repetition rate of the pulsed pump was 2 Hz higher than twice the bit rate of the input NRZ signal. The output eye pattern

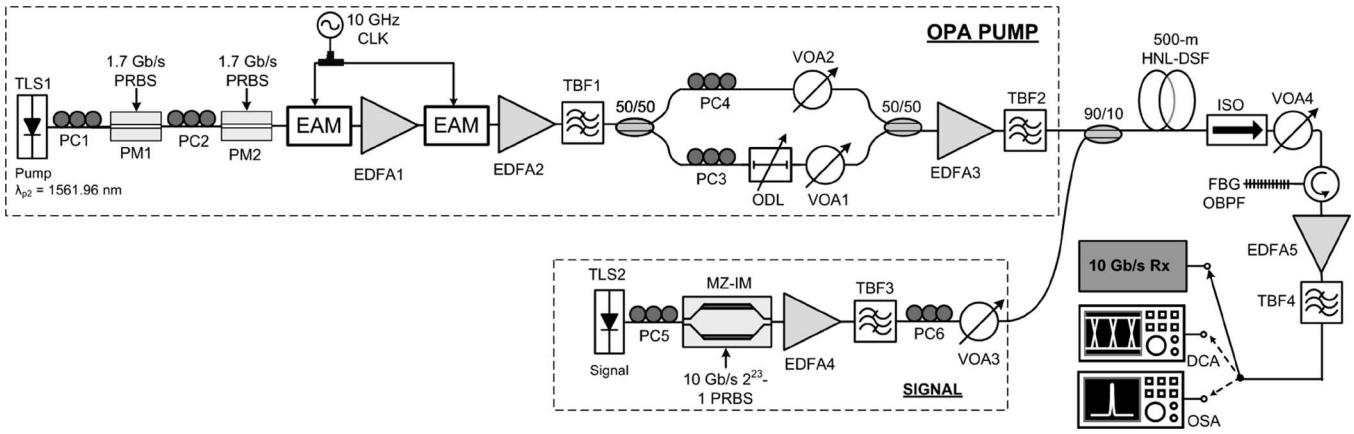

Fig. 5. Setup for performance measurements (EAM, electroabsorption modulator; ODL, optical delay line; MZ-IM, Mach–Zehnder intensity modulator; FBG-OBPF, fiber Bragg grating optical bandpass filter; DCA, digital communication analyzer).

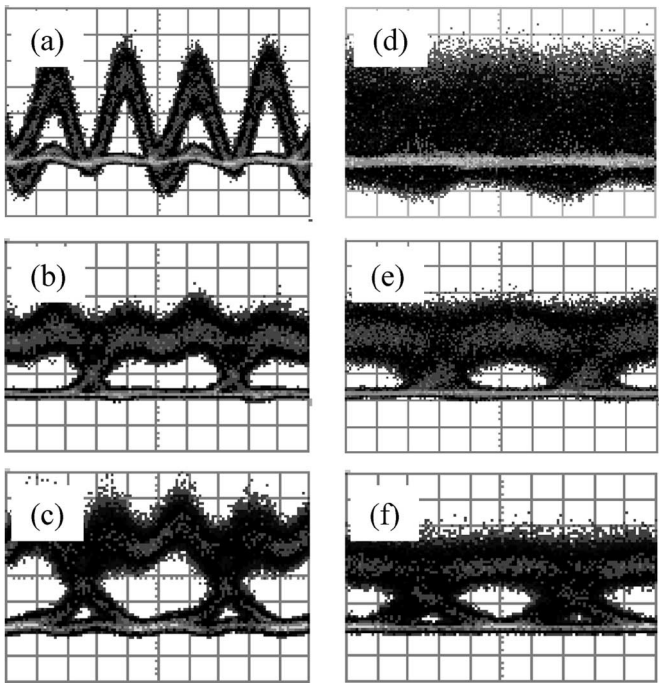

Fig. 6. Eye patterns for the pulsed-pump OPA. Left: synchronous pump. Right: asynchronous pump.

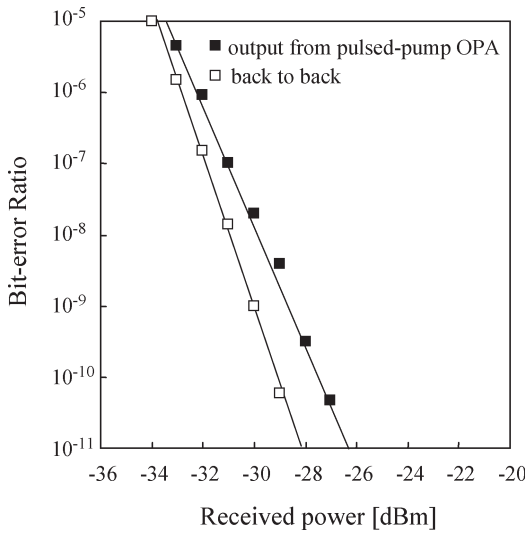

Fig. 7. BER performance of 10-Gb/s NRZ signal amplified by the 20-GHz pulsed-pump OPA, followed by a narrowband optical filter.

from the asynchronous pulsed-pump OPA, triggered by the signal clock, is shown in Fig. 6(d). The eye opening for the signal recovered by the optical FBG filter is shown in Fig. 6(e). Fig. 6(f) shows the eye opening when an electrical lowpass filter was used. Asynchronous pumping is not expected to induce additional penalty because the only limitation of the proposed technique is that the repetition rate of the pulsed pump should be higher than twice the bit rate of the input signal. This is better understood in the frequency domain, as depicted in Fig. 1(e) and (f). A sufficiently narrowband optical filter at the output can recover the original (amplified) signal, irrespective of any pump and signal synchronization mismatch.

V. Discussion

We have proposed and experimentally verified that the use of a high-repetition-rate pump OPA, followed by a narrowband optical filter, can provide significant improvements in gain and gain bandwidth, compared to a CW pump. Naturally, one should expect that these improvements are subject to tradeoffs with some other aspects of the OPA performance.

An important tradeoff is with usable bandwidth. The gain spectra shown in Sections II and III were obtained by changing the wavelength of a single input signal. Unfortunately, they cannot be used for simultaneously amplifying a number of channels placed very close together as in a dense wavelength-division multiplexed (DWDM) system. The reason for this is that the pulsed-pump OPA generates replicas of the spectrum of each signal, as shown in Fig. 1 (where they are spaced 20 GHz apart). Hence, if we attempted to transmit two different input signals spaced by 20 GHz at the OPA output, their spectra would strongly overlap and we would experience a large amount of crosstalk when selecting either output signal. We could still simultaneously send several input signals, but they should be spaced far apart enough for this type of crosstalk to be negligible. This would prevent placing signals as close as those in DWDM and would thus lead to a reduction in bandwidth utilization compared to an OPA with a CW pump.

According to Nyquist's sampling theory, the repetition rate of the pump pulses should be higher than twice the signal bit rate. In spite of the fact that our sampling rate was at the Nyquist limit, a clear eye opening was demonstrated. A higher repetition rate for the pump pulses will lead to a better recovered waveform.

An interesting aspect of using a pulsed pump is that the SBS threshold is increased, compared to a CW pump with the same power, because the total power is then spread over several frequency components. In particular, when the initial pump consists of two CW waves, the increase is at least 3 dB because each wave has half the total power. In a high-gain OPA, pump self-phase modulation (SPM) further broadens the spectrum [10], reducing the power of the initial waves and further increasing the SBS threshold. This feature should make it easier to obtain gains of the order of 60 dB or higher, which is difficult to do with CW OPAs [12].

Dispersion of the associated pump pulses and walk-off effects between pump pulses and signal pulses has not been accounted for in our analysis mainly because these effects are quite small at the wavelengths of operation for typical highly nonlinear fibers used for OPA devices. For example, if we assume that the pump and signal are at 1562 and 1542 nm, respectively, then the walk-off parameter between the pump and signal is $d_{p-s} = |\beta_1(\lambda_p) - \beta_1(\lambda_s)| \approx |D(\lambda_c)| \cdot |\lambda_p - \lambda_s|$, where β_1 is the first-order derivative of the propagation constant, D is the chromatic dispersion coefficient in ps/(nm · km), and $\lambda_c = (\lambda_s + \lambda_p)/2 = 1552$ nm. Based on the parameters of the fiber used, the walk-off parameter value is $d_{p-s} \approx 5.5$ ps/km. If we assume pump pulses of 15-ps width (same as the pulses in our experiment), the walk-off length would be $L_w = 15\ \text{ps}/(5.5\ \text{ps/km}) = 2.7\ \text{km} \gg L_{\text{HNLF\_OPA}} = 0.5\ \text{km}$. Thus, we do not expect the pulse walk-off to play an important role in the performance of the proposed configuration. Any fluctuations in the dispersion along the fiber (e.g., zero-dispersion wavelength fluctuations) would affect the walk-off parameter d_{s-p}, which is by itself too small to induce performance degradation. Dispersion effects on the width of the pump pulses in the HNLF can also be neglected. The dispersion at the wavelength of the pump is $D(\lambda_p) = 0.026$ ps/(nm · km), which corresponds to $\beta_2(\lambda_p) = 0.033\ \text{ps}^2/\text{km}$. Thus, for 15-ps pulsewidth, the dispersion length for the pump pulses is

$$\begin{aligned} L_{D\_\text{pump}} &= \frac{T_p^2}{|\beta_2(\lambda_p)|} \\ &= \frac{(15\ \text{ps})^2}{0.033\ \text{ps}^2/\text{km}} \approx 6800\ \text{km} \gg L_{\text{HNLF\_OPA}} \\ &= 0.5\ \text{km}. \end{aligned}$$

VI. Conclusion

A high-repetition-rate pulsed-pump OPA followed by a narrow optical filter was introduced to amplify communication signals with arbitrary modulation formats. This arrangement can provide larger gain and gain bandwidth than the same OPA with a CW pump of the same power. We experimentally confirmed the concept by demonstrating a gain increase from 19.7 to 29.2 dB and a bandwidth increase by switching from a CW pump to a modulated one. Low-penalty amplification was obtained for 10-Gb/s NRZ signals using a 20-GHz pulsed pump. The proposed concept may find applications in the transparent amplification of wideband signals.

Acknowledgment

The authors would like to thank Dr. M. Onishi of Sumitomo Electric Industries, Ltd. for providing the HNL-DSF, OIDA for providing the high-power EDFA and filter, and Sprint Advanced Technology Labs for the loan of equipment.

References

[1] M. C. Ho, K. Uesaka, M. E. Marhic, Y. Akasaka, and L. G. Kazovsky, "200 nm-bandwidth fiber optical amplifier combining parametric and Raman gain," *J. Lightw. Technol.*, vol. 19, no. 7, pp. 977–981, Jul. 2001.

[2] M. E. Marhic, K. K.-Y. Wong, and L. G. Kazovsky, "Wideband tuning of the gain spectra of one-pump fiber optical parametric amplifiers," *IEEE J. Sel. Topics Quantum Electron.*, vol. 10, pp. 1133–1141, Sep.-Oct. 2004.

[3] M. E. Marhic, N. Kagi, T. K. Chiang, and L. G. Kazovsky, "Broadband fiber optical parametric amplifiers," *Opt. Lett.*, vol. 21, no. 8, pp. 573–575, Apr. 1996.

[4] J. Hansryd and P. A. Andrekson, "Broad-band continuous-wave-pumped fiber optical parametric amplifier with 49-dB gain and wavelength-conversion efficiency," *IEEE Photon. Technol. Lett.*, vol. 13, no. 3, pp. 194–196, Mar. 2001.

[5] M. E. Marhic, K. K. Y. Wong, G. Kalogerakis, and L. G. Kazovsky, "Toward practical fiber optical parametric amplifiers and oscillators," *Opt. Photon. News*, vol. 15, no. 9, pp. 20–25, Sep. 2004.

[6] M.-C. Ho, "Fiber optical parametric amplifiers and their applications in optical communication systems," Ph.D. dissertation, Dept. Elect. Eng., Stanford Univ., Stanford, CA, 2001.

[7] K. Uesaka, K. K.-Y. Wong, M. E. Marhic, and L. G. Kazovsky, "Wavelength exchange in a highly-nonlinear dispersion-shifted fiber: Theory and experiments," *IEEE J. Sel. Topics Quantum Electron.*, vol. 8, no. 3, pp. 560–568, May/Jun. 2002.

[8] A. Mussot, E. Lantz, T. Sylvestre, H. Maillotte, A. Durécu-Legrand, C. Simonneau, and D. Bayart, "Zero-dispersion wavelength mapping of a highly nonlinear optical fibre-based parametric amplifier," presented at the Eur. Conf. Optical Communication (ECOC), Stockholm, Sweden, 2004, Paper Tu3.3.7.

[9] OptSim, distributed by RSoft. [Online] Available: http://www.rsoftdesign.com/

[10] A. Boskovic, S. V. Chernikov, J. R. Taylor, L. Gruner-Nielsen, and O. A. Levring, "Direct continuous-wave measurement of n_2 in various types of telecommunication fiber at 1.55 μm," *Opt. Lett.*, vol. 21, no. 24, pp. 1966–1968, Dec. 1996.

[11] K. Inoue and T. Mukai, "Experimental study on noise characteristics of a gain-saturated fiber optical parametric amplifier," *J. Lightw. Technol.*, vol. 20, no. 6, pp. 969–974, Jun. 2002.

[12] K. K. Y. Wong, K. Shimizu, K. Uesaka, G. Kalogerakis, E. Marhic, and L. G. Kazovsky, "Continuous-wave fiber OPA with 60 dB gain using a novel two-segment design," *IEEE Photon. Technol. Lett.*, vol. 15, no. 12, pp. 1707–1709, Dec. 2003.

Georgios Kalogerakis (S'02) received the B.E. degree in electrical and computer engineering from the National Technical University of Athens, Greece, in 2001 and the M.S. degree in electrical engineering from Stanford University, Stanford, CA, in 2003. He is currently working toward the Ph.D. degree in electrical engineering at Stanford University.

He is currently a member of the Photonics and Networking Research Laboratory, Stanford University. His research interests include fiber nonlinearity, fiber optical parametric amplifiers, and high-speed optical transmission systems.

Mr. Kalogerakis is a member of the IEEE Lasers and Electro-Optic Society.

Michel E. Marhic (M'79–SM'89) received the Diplome D'Ingenieur degree from Ecole Superieure D'Electricite, France, the M.S. degree from Case Western Reserve University, Cleaveland, OH, and the Ph.D. degree from University of California, Los Angeles, all in electrical engineering.

He is currently a Consulting Professor with the Department of Electrical Engineering, Stanford University, Stanford, CA. He was with the Faculty of the Department of Electrical Engineering, Northwestern University (1974–1998) and on sabbatical leaves at University of South Carolina (1979–1980) and Stanford University (1984–1985 and 1993–1994). He cofounded Holicon, Holographic Industries, and OPAL Laboratories. He authored or coauthored over 240 journal and conference papers and is the holder of eight patents. Over the past 25 years, his research interests have been applied optics, including nonlinear interactions in plasmas; optical fiber measurements; hollow infrared waveguides; holography and phase conjugation; and fiber networks. Over the past ten years, his research interests have been focused on optical communication systems and nonlinear optical interactions in fibers.

Dr. Marhic was a recipient of the Ameritech Research Professorship (1990–1991) from the Institute for Modern Communications. He is a member of the Optical Society of America (OSA) and an Eminent Member of Tau Beta Pi.

Leonid G. Kazovsky (M'80–SM'83–F'91) has been a Professor of electrical engineering with Stanford University, Stanford, CA, since 1990. After joining Stanford University, he founded and led the Optical Communication Research Laboratory. Prior to joining Stanford University, he was with Bellcore (now Telcordia), where he worked on wavelength-division multiplexing and high-speed and coherent optical fiber communication systems. While on Bellcore assignments or sabbatical leaves from Stanford, he worked for the Heinrich Hertz Institute, Berlin, Germany; Hewlett-Packard Research Laboratories, Bristol, U.K.; and Technical University of Eindhoven, The Netherlands. Through research contracts, consulting engagements, and other arrangements, he worked with many industrial companies, such as Sprint, DEC, GTE, AT&T, IVP, Lucent, Hitachi, KDD, Furukawa, Fujitsu, Optivision, and Perimeter, and U.S. Government agencies, such as NSF, DARPA, Air Force, Navy, Army, and BMDO. During 1998–1999, he took a one-year leave from Stanford University and launched a start-up company now known as Alidian Networks, where he serves on the Board of Directors. He authored or coauthored two books, about 150 journal technical papers, and a similar amount of conference papers.

Prof. Kazovsky serves or served on the Editorial Boards of leading journals (IEEE TRANSACTIONS ON COMMUNICATIONS, IEEE PHOTONICS TECHNOLOGY LETTERS, *Wireless Networks*) and on Program Committees of leading conferences (OFC, CLEO, LEOS, SPIE, and GLOBECOM). He also served various IEEE and IEE transactions, proceedings, and journals, as a Reviewer; funding agencies (NSF, OFC, ERC, NRC, etc.); and publishers (Wiley, MacMillan, etc.). He is a Fellow of the Optical Society of America (OSA).

Photographs and biographies of **Katsuhiro Shimizu**, **Kenneth Kin-Yip Wong**, and **Katsumi Uesaka** not available at the time of publication.